J|A|C|S
ARTICLES
Published on Web 09/11/2004

Electrochemically Controlled Chemically Reversible Transformation of α-Tocopherol (Vitamin E) into Its Phenoxonium Cation

Leodrina L. Williams and Richard D. Webster*

Contribution from the Research School of Chemistry, Australian National University, Canberra ACT 0200, Australia

Received June 8, 2004; E-mail: webster@rsc.anu.edu.au

Abstract: α-Tocopherol (α-TOH) can be electrochemically oxidized in CH_3CN containing Bu_4NPF_6 in a chemically reversible two-electron/one-proton (ECE) process to form the phenoxonium cation (α-TO^+) that is stable for at least several hours at 243 K. In the presence of up to ~1% CF_3SO_3H, α-TO^+ exists in equilibrium with the α-tocopherol cation radical (α-$TOH^{+\bullet}$), whereas at concentrations between ~1−3% CF_3SO_3H the electrochemical oxidation of α-TOH occurs by close to one-electron to form α-$TOH^{+\bullet}$. α-$TOH^{+\bullet}$ can be further oxidized in a one-electron process to form the α-tocopherol dication (α-TOH^{2+}). The identity and stability of the phenolic cationic compounds were determined by a combination of electrochemical (cyclic voltammetry and controlled potential electrolysis) and in situ spectroscopic (UV−vis−NIR, FTIR, EPR, and NMR) analysis.

1. Introduction

α-TOH is the most naturally abundant, fully methylated, and biologically active of the four (α, β, γ, and δ) structurally related phenolic (PhOH) compounds that are labeled vitamin E.[1] The electrochemical behavior of α-TOH is expected to be similar to other phenolic compounds, which display a richness of voltammetric responses depending on the solution acidity and the nature of substituents in the 2-, 4-, and 6- positions.[2,3] The theoretical sequence of electron and proton transfers associated with α-TOH (and related species) are given in Scheme 1,[2−5] although to date, there is little experimental data that confirms the identity or stability of the phenoxonium ion (α-TO^+) or dication (α-TOH^{2+}).[5] The focus of this study is to establish conditions that enable the electrochemical generation of the intermediate species and to determine their stability on the CV (seconds) and electrolysis (hours) time-scales. Considering the importance of vitamin E in biological systems (both plant and animal), it is of interest to determine the degree of chemical reversibility that exists between α-TOH and the relatively rare (among all phenolic compounds) potential cationic compounds, α-$TOH^{+\bullet}$, α-TOH^{2+}, and α-TO^+, particularly in a pH neutral environment.

Figure 1 illustrates the cyclic voltammetric behavior of α-TOH compared to other simple phenols in neutral and mildly basic conditions. In aprotic organic solvents, most substituted phenols are oxidized at positive potentials by two-electrons [Figure 1 (black lines)]. The addition of an equivalent molar amount of an organic soluble base, such as Et_4NOH to the acetonitrile solutions, immediately forms the phenolate anions (PhO^-) that undergo one-electron oxidation between ~1.2−1.8 V more negative than their associated phenols (reactions 1 and 2) [Figure 1 (blue lines)].[2,6−9]

$$PhOH + Et_4NOH \rightleftharpoons PhO^- + Et_4N^+ + H_2O \qquad (1)$$

$$PhO^- \rightleftharpoons PhO^{\bullet} + e^- \qquad (2)$$

In pure aprotic solvents such as acetonitrile or dimethylformamide, the phenoxyl radicals prepared by electro-oxidation of the phenolate anions have been shown to undergo a range of reactions, mainly involving dimerization and disproportionation.[2,6] Electrochemical studies have shown that phenoxyl radicals with bulky substituents in the 2-, 4-, and 6- positions are the most stable toward irreversible bimolecular reactions, although rapid *reversible* reactions to form dimers are common. CV experiments performed on solutions of 2,4,6-tri-*tert*-butylphenolate [Figure 1b (blue line)] and 2,6-di-*tert*-butyl-4-methoxyphenolate [Figure 1c (blue line)] indicate that the associated phenoxyl radicals are the most stable of the compounds shown in Figure 1. Bulk electrolysis, EPR and FTIR

(1) Burton, G. W.; Ingold, K. U. *Acc. Chem. Res.* **1986**, *19*, 194−201.
(2) Hammerich, O.; Svensmark, B. In *Organic Electrochemistry*, 3rd ed.; Lund, H., Baizer, M. M., Eds.; Marcel Dekker: New York, 1991; Chapter 16.
(3) (a) Rieker, A.; Beisswenger, R.; Regier, K. *Tetrahedron*, **1991**, *47*, 645−654. (b) Eickhoff, H.; Jung, G.; Rieker, A. *Tetrahedron*, **2001**, *57*, 353−364.
(4) Parker, V. D. *J. Am. Chem. Soc.* **1969**, *91*, 5380−5381.
(5) Svanholm, U.; Bechgaard, K.; Parker, V. D. *J. Am. Chem. Soc.* **1974**, *96*, 2409−2413.
(6) (a) Richards, J. A.; Whitson, P. E.; Evans, D. H. *J. Electroanal. Chem.* **1975**, *63*, 311−327. (b) Richards, J. A.; Evans, D. H. *J. Electroanal. Chem.* **1977**, *81*, 171−187. (c) Evans, D. H.; Jimenez, P. J.; Kelly, M. J. *J. Electroanal. Chem.* **1984**, *163*, 145−157. (d) Hapiot, P.; Pinson, J. *J. Electroanal. Chem.* **1993**, *362*, 257−265.
(7) Nanni, E. J., Jr.; Stallings, M. D.; Sawyer, D. T. *J. Am. Chem. Soc.* **1980**, *102*, 4481−4485.
(8) Webster, R. D. *Electrochem. Commun.* **1999**, *1*, 581−584.
(9) (a) Webster, R. D. *Electrochem. Commun.* **2003**, *5*, 6−11. (b) Müller, E.; Rieker, A.; Scheffler, K. *Liebigs Ann. Chem.* **1961**, *645*, 92−100.

Scheme 1. One Resonance Structure Is Displayed for Each Compound

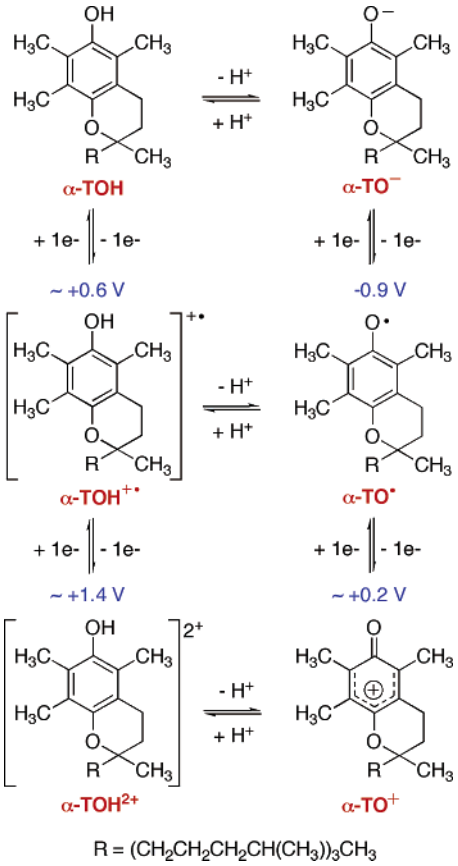

The listed potentials (vs Fc/Fc^+) were obtained by voltammetry and are the approximate values necessary to bring about oxidation of the phenolic compounds but do not necessarily correspond to the formal potential (see text).

studies have shown that the neutral radicals are stable for at least several hours at room temperature in acetonitrile,[9a] and 2,4,6-tri-*tert*-butylphenoxyl has been isolated as a solid.[9b] The methyl groups in the 2- and 6- positions do not provide sufficient steric hindrance to stabilize the α-TO• radical for long periods, hence there is only a small reverse peak observed in CV experiments on the phenolate anion [Figure 1d (blue line)] at mM concentrations.[7,8]

The primary interest in α-TO• relates to its biological function in mammalian tissues as a chain breaking antioxidant, inhibiting lipid peroxidation (autoxidation) by two principal steps (reactions 3 and 4).[1] First, α-TOH reacts with an oxidized site on a lipid cell wall (LOO•) to yield a molecule of lipid hydroperoxide (LOOH) and the tocopheroxyl radical (α-TO•) (reaction 3). Second, the α-TO• radical reacts with another LOO• radical (reaction 4), so that overall one α-TOH molecule is able to inhibit two LOO• sites.

$$\text{LOO}^\bullet + \alpha\text{-TOH} \rightarrow \text{LOOH} + \alpha\text{-TO}^\bullet \quad (3)$$

$$\text{LOO}^\bullet + \alpha\text{-TO}^\bullet \rightarrow (\alpha\text{-TO})\text{OOL} \quad (4)$$

$$\alpha\text{-TO}^\bullet + \alpha\text{-TO}^\bullet \rightarrow \text{nonradical products} \quad (5)$$

In organic solvents the principal mode of decomposition of α-TO• radicals occurs via a bimolecular self-reaction, where an H-atom is transferred from the 5-methyl group of one radical

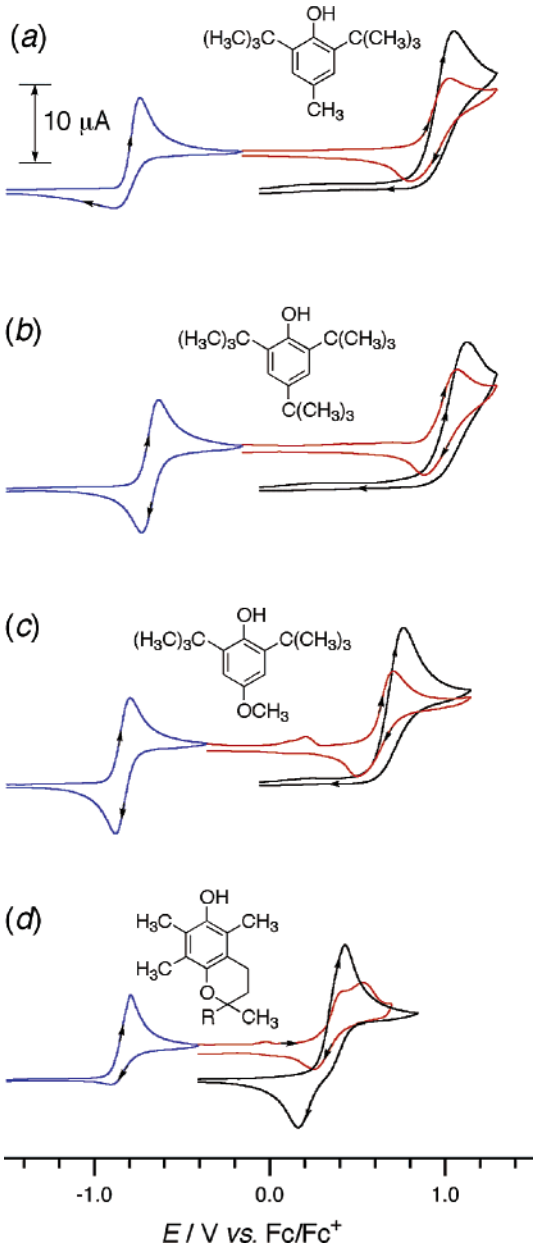

Figure 1. Cyclic voltammograms recorded at 293 K at a scan rate of 0.1 V s^{-1} with a 1.6 mm diameter Pt electrode in CH_3CN with 0.25 M Bu_4NPF_6 and 2.0 mM substrate. (Black line) The two-electron oxidation of the substituted phenols (PhOH). (Blue line) The one-electron oxidation of the phenolate anions (PhO^-) prepared by the addition of 2 mM Et_4NOH to the same solutions of PhOH. (Red line) The further oxidation of the phenoxyl radicals (PhO•).

to the phenoxyl oxygen atom of another radical (reaction 5).[10] Kinetic data associated with the reaction of α-TO• under different conditions have been extensively studied, often using UV−vis and/or EPR spectroscopies as the method of analysis.[10,11] The second-order rate constant for reaction 5 has been estimated to be 7.1×10^3 L mol^{-1} s^{-1} at 310 K in chlorobenzene[10] and 3×10^3 L mol^{-1} s^{-1} at 293 K in CH_3CN,[8] which is slow enough (at μM level concentrations) to have enabled detailed characterization of the radical by EPR spectroscopy.[12]

The cation radical ($\alpha\text{-TOH}^{+\bullet}$) formed by one-electron oxidation of α-TOH (Scheme 1) has been shown to exist by EPR spectroscopy in organic solvents containing a strong acid

(10) Bowry, V. W.; Ingold, K. U. *J. Org. Chem.* **1995**, *60*, 5456−5467.

mixture,[5,13] and as a transitory species identified in pulse radiolysis studies.[14] The stability of α-$TOH^{+\bullet}$ in a strong acid environment is expected based on cyclic voltammetric studies on other more simple phenols, which have shown that the two-electron oxidation process changes to a one-electron chemically reversible process in strong acid conditions at low temperatures, showing improved stability of the monocation radicals.[15] In neutral media, phenolic cation radicals are thought to be too acidic to be stable,[2] although cation radicals of model vitamin E compounds have also been proposed to exist as moderately stable species at temperatures below 263 K via oxidation with $AlCl_3$ in CH_2Cl_2.[16] The dication of a vitamin E model compound (α-TOH^{2+}) has been proposed to exist under special conditions in organic solvents containing strong acid, or generated by reaction of α-TOH with antimony pentachloride in dichloromethane.[5]

Phenoxyl radicals are oxidized at an apparently similar electrode potential to that of their associated phenols [Figure 1 (red lines)]. Nevertheless, there are difficulties in assigning the true electrode potentials of phenols from cyclic voltammograms since the homogeneous chemical processes that accompany the heterogeneous electron transfer steps can shift the oxidation wave of the phenol to substantially less positive potentials. Since the potential of the voltammetric wave is influenced by the kinetics of the homogeneous reactions, the peak potential (or half-wave potential) does not correspond to the thermodynamic formal potential (E^0).[2] The anodic peak currents associated with oxidation of the phenoxyl radicals shown in Figure 1 are close to the anodic peak currents due to oxidation of the phenolate anions, suggesting that the phenoxyl radical oxidation also occurs via a one-electron process, most likely to form the phenoxonium cations (PhO^+). The presence of a reverse peak in CV experiments during the oxidation of the phenoxyls suggests that the phenoxonium ions are moderately stable (at least on the CV time-scale). This observation is particularly significant for the species in Figure 1b and Figure 1c (blue lines) where the phenoxyl radicals are themselves very stable, so that the second one-electron-transfer process [Figure 1 (red lines)] is not affected by possible decomposition products of the first electron-transfer reaction [that may occur for the species in Figure 1, parts a and d (blue lines)]. The splitting in the peak at ~0.5 V vs. Fc/Fc^+ during the oxidation of the α-$TO^\bullet$ [Figure 1d (red line)] is likely to be due to an additional product caused by decomposition of the α-$TO^\bullet$ radical (which forms *via* the first one-electron oxidation of α-TO^-). The extra signal detected in the oxidation scan for 2,6-di-*tert*-butyl-4-methoxyphenolate at ~0.1 V *vs.* Fc/Fc^+ is possibly due to an adsorption process [Figure 1c (red line)]. It is surprising that the stability of the phenoxonium ions appears to be influenced by whether the electron-transfer mechanism begins with PhOH [Figure 1 (black lines)] or with the $PhO^\bullet$ [Figure 1 (red lines)].

The principal difference in the electrochemical responses of vitamin E and the other compounds in CH_3CN (containing Bu_4NPF_6) displayed in Figure 1 (black lines) is that a reverse reduction peak is detected during CV experiments on α-TOH. This study is primarily concerned with identifying the intermediate species produced during the oxidation of α-TOH in CH_3CN and determining whether the reverse reduction peak is associated with regenerating the starting material. The cyclic voltammetric response observed for α-TOH in neutral organic media is similar to that seen for 2,6-di-*tert*-butyl-4-(4-dimethylaminophenyl)phenol, where it was shown that the reverse peak detected during CV experiments was due to reduction of the phenoxonium ion that formed rapidly following two-electron oxidation of the phenol.[17] It has been noted that the presence of bulky electron donating substituents in the 4-position are critical for the stabilization of phenoxonium cations,[2,5,17,18] with 2,6-di-*tert*-butyl-4-(4-dimethylaminophenyl)phenoxonium found to be sufficiently stable to be isolated as a solid salt.[17] However, the bulkiness cannot be the only factor since 2,4,6-tri-*tert*-butylphenol does not readily lead to a stable phenoxonium ion following oxidation [Figure 1b (black line)].

2. Experimental Section

2.1. Reagents. Vitamin E (97%), 2,6-di-*tert*-butyl-4-methylphenol (99%), 2,6-di-*tert*-butyl-4-methoxyphenol (97%), 2,4,6-tri-*tert*-butylphenol (98%), Et_4NOH (20 wt. % in water), and CF_3SO_3H (98%) were obtained from Aldrich and stored in the dark under nitrogen. Bu_4NPF_6 was prepared and purified by standard methods,[19] dried under vacuum at 413 K for 72 h and stored under nitrogen. HPLC grade acetonitrile (EM Science) was purified and dried according to a published procedure,[20] stored over calcium hydride (under nitrogen) and distilled immediately prior to use. Acetonitrile-d_3, (99.8% D, Aldrich) for NMR experiments was stored over 4 Å molecular sieves under nitrogen.

2.2. Apparatus. Voltammetric experiments were conducted with a computer controlled Eco Chemie μAutolab III potentiostat. Bulk electrolyzed solutions of vitamin E were prepared in a divided controlled potential electrolysis cell separated with a porosity no. 5 (1.0−1.7 μm) sintered glass frit. The working and auxiliary electrodes were identically sized Pt mesh plates symmetrically arranged with respect to each other with an Ag wire reference electrode (isolated by a salt bridge) positioned to within 2 mm of the surface of the working electrode. The electrolysis cell was jacketed in a glass sleeve and cooled to 243 K using a Lauda RL6 variable temperature methanol-circulating bath. The volumes of both the working and auxiliary electrode compartments were approximately 20 mL each. The α-TOH solution in the working electrode compartment was simultaneously deoxygenated and stirred using bubbles of argon gas, while the auxiliary electrode compartment was

(11) For examples see; (a) Packer, J. E.; Slater, T. F.; Willson, R. L. *Nature*, **1979**, *278*, 737−738. (b) Niki, E.; Tsuchiya, J.; Tanimura, R.; Kamiya, Y. *Chem. Lett.* **1982**, 789−792. (c) Scarpa, M.; Rigo, A.; Maiorino, M.; Ursini, F.; Gregolin, C. *Biochim. Biophys. Acta*, **1984**, *801*, 215−219. (d) Severcan, F.; Cannistraro, S. *Chem. Phys. Lipids*, **1990**, *53*, 17−26. (e) Ingold, K. U.; Bowry, V. W.; Stocker, R.; Walling, C. *Proc. Natl. Acad. Sci. U.S.A.*, **1993**, *90*, 45−49. (f) Iwatsuki, M.; Tsuchiya, J.; Komuro, E.; Yamamoto, Y.; Niki, E. *Biochim. Biophys. Acta*, **1994**, *1200*, 19−26. (g) Stoyanovsky, D. A.; Osipov, A. N.; Quinn, P. J.; Kagan, V. E. *Arch. Biochem. Biophys.* **1995**, *323*, 343−351. (h) Valgimigli, L.; Banks, J. T.; Ingold, K. U.; Lusztyk, J. *J. Am. Chem. Soc.* **1995**, *117*, 9966−9971. (i) Valgimigli, L.; Lucarini, M.; Pedulli, G. F.; Ingold, K. U. *J. Am. Chem. Soc.* **1997**, *119*, 8095−8096.

(12) (a) Kohl, D. H.; Wright, J. R.; Weissman, M. *Biochim. Biophys. Acta*, **1969**, *180*, 536−544. (b) Ozawa, T.; Hanaki, A.; Matsumoto, S.; Matsuo, M. *Biochim. Biophys. Acta*, **1978**, *531*, 72−78. (c) Mukai, K.; Tsuzuki, N.; Ishizu, K.; Ouchi, S.; Fukuzawa, K. *Chem. Phys. Lipids* **1981**, *29*, 129−135. (d) Matsuo, M.; Matsumoto, S.; Ozawa, T. *Org. Magn. Reson.* **1983**, *21*, 261−264.

(13) Lehtovuori, P.; Joela, H. *Phys. Chem. Chem. Phys.* **2002**, *4*, 1928−1933.

(14) (a) Parker, A. W.; Bisby, R. H. *J. Chem. Soc., Faraday Trans.* **1993**, *89*, 2873−2878. (b) Edge, R.; Land, E. J.; McGarvey, D.; Mulroy, L.; Truscott, T. G. *J. Am. Chem. Soc.* **1998**, *120*, 4087−4090.

(15) (a) Hammerich, O.; Parker, V. D.; Ronlán, A. *Acta Chem. Scand. B*, **1976**, *30*, 89−90. (b) Hammerich, O.; Parker, V. D. *Acta Chem. Scand. B*, **1982**, *36*, 63−64.

(16) Mukai, K.; Tsuzuki, N.; Ishizu, K.; Ouchi, S.; Fukuzawa, K. *Chem. Phys. Lipids*, **1984**, *35*, 199−208.

(17) (a) Speiser, B.; Rieker, A. *J. Chem. Res. (S)*, **1977**, 314−315. (b) Speiser, B.; Rieker, A. *J. Electroanal. Chem.* **1979**, *102*, 373−395. (c) Speiser, B.; Rieker, A. *J. Electroanal. Chem.* **1980**, *110*, 231−246.

(18) Nilsson, A.; Palmquist, U.; Ronlán, A.; Parker, V. D. *J. Am. Chem. Soc.* **1975**, *97*, 3540−3541.

(19) Fry, A. J.; Britton, W. E. In *Laboratory Techniques in Electroanalytical Chemistry*; Kissinger, P. T., Heineman, W. R., Eds.; Marcel Dekker: New York, 1984; Chapter 13.

(20) Walter, M.; Ramaley, L. *Anal. Chem.* **1973**, *45*, 165−166.

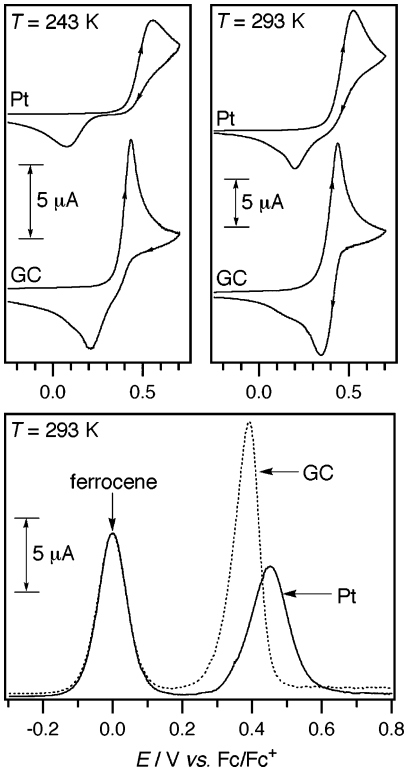

Figure 2. Cyclic (above) (v = 0.1 V s^{-1}) and square-wave (below) voltammograms recorded at 243 and 293 K with 1.0 mm diameter GC and Pt electrodes in CH_3CN with 0.5 M Bu_4NPF_6 and 3.3 mM α-TOH.

purged with bubbles of oxygen gas that served as the electron accepting reagent through the cathodic reduction of dissolved molecular oxygen ($O_2 + 1e^- \leftrightarrow O_2^{-\bullet}$). The number of electrons transferred during the bulk oxidation process was calculated from

$$N = Q/nF \quad (6)$$

where N = no. of moles of starting compound, Q = charge (coulombs), n = no. of electrons, and F is the Faraday constant (96 485 C mol^{-1}).

UV−vis−NIR experiments were performed on a Varian Cary 5E spectrophotometer, FTIR experiments were conducted with a Mettler Toledo ReactIR 4000 spectrometer utilizing a diamond composite attenuated total reflection (ATR) probe, NMR experiments were performed with a Varian INOVA 500 MHz ^{1}H NMR spectrometer and EPR experiments were conducted on an Bruker ER 200D X-band spectrometer with a rectangular TE_{102} cavity. The electrochemical cells used to perform the in situ UV−vis−NIR,[21] ATR-FTIR,[22] NMR[23] and EPR[21,24] experiments have been described previously.

3. Results and Discussion

3.1. Electrochemistry. Cyclic voltammograms of solutions of α-TOH recorded on glassy carbon (GC) and Pt electrodes at 293 and 243 K are shown in Figure 2. The anodic (E_p^{ox}) to cathodic (E_p^{red}) peak separations (ΔE_{pp}) obtained on both electrodes were several hundred mV higher than expected for a two-electron electrochemically reversible process (30 mV at 298 K). The ΔE_{pp}-values were larger on Pt compared to GC electrodes, and increased as the temperature was lowered (especially on Pt) by a greater amount than could be accounted for by effects of uncompensated solution resistance. Varying the scan rate between 0.1 and 5 V s^{-1} resulted in the ΔE_{pp}-values increasing by a small amount that could be attributed solely to the effects of solution resistance,[25] while the shapes of the E_p^{ox} and E_p^{red} peaks were more complex (especially on GC) than could be explained by slow rates of heterogeneous electron transfer. On GC, the anodic peak current (i_p^{ox}) was greater than that observed at an identically sized Pt electrode. Furthermore, on GC the current−potential trace observed for the forward scan in the region immediately before and after the E_p^{ox}-value was particularly steep, more so than expected for a simple diffusion-controlled process and suggesting adsorptive phenomena. Nevertheless, repeated cycling resulted in the voltammetric traces closely overlaying each other, suggesting that a rapid adsorption−desorption mechanism was in place on GC for the forward scan, so that the electrode surface was not becoming irreversibly fouled. Therefore, it is likely that the complicated voltammetric peak shapes and large ΔE_{pp}-values observed on both electrodes resulted from a combination of homogeneous chemical reactions following electron transfer in addition to specific solute interactions with the electrode surface.

Square-wave voltammetry (SWV) led to the detection of a symmetrically shaped peak centered at +0.45 V vs Fc/Fc^+ on Pt and a sharp peak at +0.39 V vs Fc/Fc^+ on GC (Figure 2), further illustrating the voltammetric wave shape dependence on the electrode surface. The electrode potential associated with the oxidation of the phenol is likely to be within 0.2 V more positive than the peak values obtained by CV and square-wave voltammetry (due to the follow-up chemical reactions lowering the peak potentials from the formal potentials[2]). Varying the concentration between 1 and 15 mM did not lead to a notable change in the shape of the voltammetric traces other than the expected change in peak current with concentration.

The cyclic voltammograms shown in Figure 2 do not in isolation allow the determination of whether the electron transfer reactions and chemical reactions are chemically reversible, since the reverse peak is so widely separated from the forward peak it is not obvious that the starting material is necessarily regenerated from the oxidized species. To determine the true degree of chemical reversibility, controlled potential electrolysis (CPE) experiments were performed on α-TOH at 243 K. The potential applied during CPE experiments was 150 mV more positive than the E_p^{ox}-values obtained by CV experiments, which was sufficiently positive to bring about complete oxidation of the substrate. Cyclic voltammograms performed at the start and completion of the electrolysis are shown in Figure 3a, along with the corresponding coulometry data for the oxidation (Figure 3b) and reverse reduction (Figure 3c) reactions. (The current−time traces obtained during the electrolysis appear noisy due to bubbles of gas being used to stir the solution.) The exhaustive oxidation resulted in the transfer of very close to 2 electrons per molecule (n = 1.90) after ca. 1 h (Figure 3b) and the formation of an orange-red colored solution. The CV obtained at the completion of the electrolysis showed voltammetric peaks (E_p^{ox} and E_p^{red}) in identical positions to the starting material [Figure 3a (red line)], albeit with the current values offset due to the product existing in the fully oxidized state. Applying a

(21) Webster, R. D.; Heath, G. A. *Phys. Chem. Chem. Phys.* **2001**, *3*, 2588−2594.
(22) Webster, R. D. *J. Chem. Soc., Perkin Trans. 2*, **2002**, 1882−1888.
(23) Webster, R. D. *Anal. Chem.* **2004**, *76*, 603−610.
(24) (a) Coles, B. A.; Compton, R. G. *J. Electroanal. Chem.* **1983**, *144*, 87−98. (b) Webster, R. D.; Bond, A. M.; Coles, B. A.; Compton, R. G. *J. Electroanal. Chem.* **1996**, *404*, 303−308.
(25) (a) *Digisim* by Bioanalytical Systems, Inc. (BAS), 2701 Kent Avenue, West Lafayette, IN 47906, USA. (b) Rudolph, M.; Reddy, D. P.; Feldberg, S. W. *Anal. Chem.* **1994**, *66*, 589A-600A.

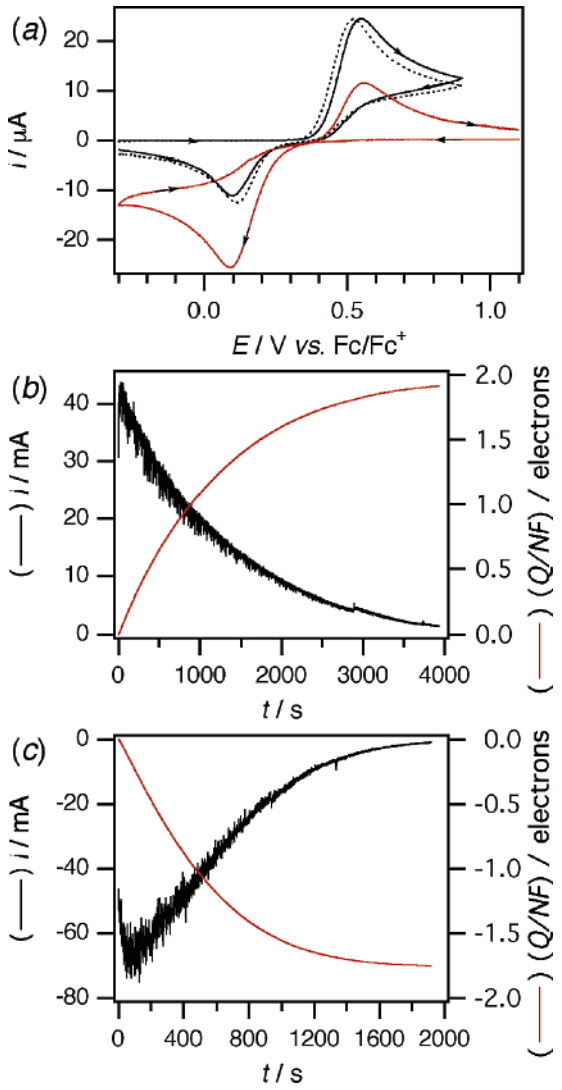

Figure 3. Voltammetric and coulometric data obtained at 243 K during the controlled potential electrolysis of 13.2 mM α-TOH in CH_3CN with 0.5 M Bu_4NPF_6. (a) Cyclic voltammograms recorded at a scan rate of 0.1 V s^{-1} with a 1.0 mm diameter Pt electrode. (Black line) Prior to the bulk oxidation of α-TOH. (Red line) After the exhaustive oxidation of α-TOH to α-TO^+. (Dashed line) After the exhaustive reduction of α-TO^+ back to α-TOH. (b) Current vs time data obtained during the exhaustive oxidation of α-TOH at 0.7 V vs Fc/Fc^+. (c) Current vs time data obtained during the reverse exhaustive reduction of α-TO^+ at 0.0 V vs Fc/Fc^+. For (*b*) and (*c*) the number of electrons transferred per molecule (*Q*/*NF*) during the CPE experiments were calculated from eq 6.

potential sufficiently negative to reduce the oxidized species (0 V vs Fc/Fc^+) resulted in the transfer of 1.75 electrons per molecule after 30 min[26] (Figure 3c), while a CV of the solution performed at the completion of the reverse electrolysis [Figure 3a (dashed line)] was almost identical to that of the starting material. The reason for the fewer number of electrons transferred on the reverse electrolysis direction may be due to some of the oxidized vitamin E having reacted with superoxide (generated at the auxiliary electrode) at the interface of the working and auxiliary electrode compartments of the electrolysis cell, which would immediately regenerate vitamin E (and 2 mols

(26) The faster conversion of the oxidized product back to the starting material (compare Figures 3b and 3c) on the CPE time-scale is most likely associated with the performance of the CPE cell and not specific to the vitamin E system, since we have observed the same type of behavior with other compounds.

Scheme 2

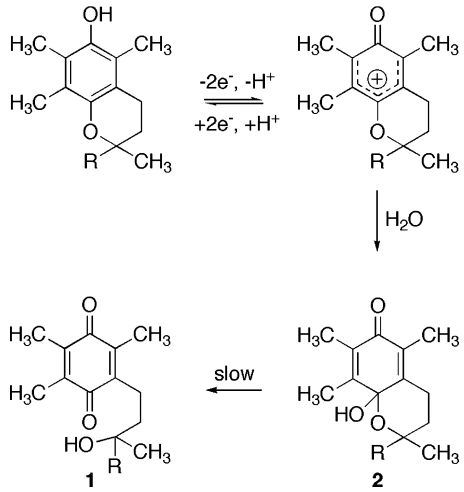

of O_2) in a thermodynamically favorable electron-transfer reaction.[27] Partial decomposition of the oxidized vitamin E is also possible, although the i_p^{ox}- and i_p^{red}-values from CV experiments at the completion of the electrolysis were very similar to those obtained from the starting material, suggesting that α-TOH is almost completely regenerated.

The CPE results prove that the two-electron oxidized intermediate is stable for at least several hours at low temperatures and confirm that the reverse reduction peak detected during CV experiments on α-TOH is associated with the reformation of the starting material. At room temperature the oxidized species is only moderately stable and decomposes within approximately 1 h of the exhaustive electrolysis. Attempts to isolate the oxidized compound were not successful, since it decomposed during the workup stage (separation from the supporting electrolyte would also be extremely difficult due to the intermediate's instability at ambient temperature in solution). Bulk oxidation of α-TOH in aqueous acetonitrile solutions has been found to form the quinone (**1**) as the long-term *stable* isolated product, through the phenoxonium and 9-hydroxy-α-tocopherone (**2**) intermediates (Scheme 2).[28] Analysis of the previous experiments performed by Parker et al.[4,5] on a model vitamin E compound in acidic conditions and by Speiser and Rieker[17] on the 2,6-di-*tert*-butyl-4-(4-dimethylaminophenyl)-phenol system, combined with the $n = 2$ values observed during the present CPE experiments, would suggest that the phenoxonium cation (rather than the dication) is the most likely candidate for the oxidized intermediate, through the series of electron transfer and proton-transfer reactions given in Scheme 1 and reaction 7, which corresponds to an ECE mechanism (where E is an electron transfer and C corresponds to a chemical step).

$$\text{α-TOH} \underset{+e}{\overset{-e}{\rightleftharpoons}} \text{α-TOH}^{+\bullet} \underset{+H^+}{\overset{-H^+}{\rightleftharpoons}} \text{α-TO}^{\bullet} \underset{+e}{\overset{-e}{\rightleftharpoons}} \text{α-TO}^{+} \qquad (7)$$

(27) Electrochemically generated superoxide is stable for several hours in dry CH_3CN containing tetraalkylammonium salts (Webster, R. D.; Bond, A. M. *J. Chem. Soc., Perkin Trans. 2*, **1997**, 1075−1079, and references therein). $E°$ for $O_2/O_2^{-\bullet} = -1.23$ V vs Fc/Fc^+ and $E°$ for α-TOH/α-TO^+ ≈ +0.6 V vs Fc/Fc^+ in CH_3CN. Therefore, $\Delta G° = -E° F \approx -180$ kJ mol^{-1} for the reaction $^1/_2$α-$TO^+ + {}^1/_2H^+ + O_2^{-\bullet} \leftrightarrow {}^1/_2$α-TOH + O_2. Many other naturally occurring reductants (such as semiquinones) should also readily react with α-TO^+.

(28) (a) Dürckheimer, W.; Cohen, L. A. *J. Am. Chem. Soc.* **1964**, *86*, 4388−4393. (b) Marcus, M. F.; Hawley, M. D. *J. Org. Chem.* **1970**, *35*, 2185−2190.

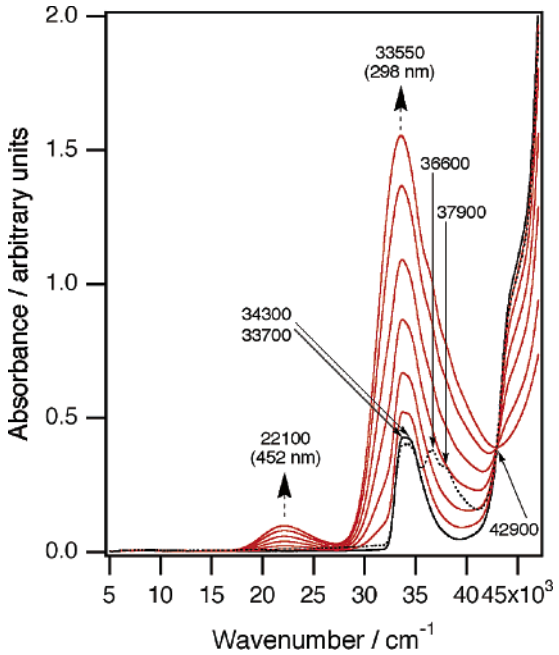

Figure 4. In situ UV−vis−NIR spectra obtained at 243 K during the oxidation of 2.1 mM α-TOH at a Pt mesh electrode in CH_3CN with 0.5 M Bu_4NPF_6. (Black line) Prior to the bulk oxidation of α-TOH. (Red line) During the oxidation of α-TOH to α-TO^+ at 0.7 V vs Fc/Fc^+. (Dashed line) After the exhaustive reduction of α-TO^+ back to α-TOH at 0.0 V vs Fc/Fc^+.

To our knowledge, the only spectroscopic evidence for the existence of α-TO^+ has come from ex situ UV−vis experiments in acid conditions on the vitamin E model compound (where the phytyl "tail" was replaced with a methyl group).[5]

3.2. UV−Vis−NIR Spectroscopy. Progressive UV−vis−NIR spectra obtained during the two-electron in situ electrolysis of 2.1 mM α-TOH in an optically transparent thin layer electrochemical (OTTLE) cell at 243 K are shown in Figure 4. The spectrum of α-TOH shows an absorbance with closely spaced maxima at 33 700 and 34 300 cm^{-1} [Figure 4 (black line)].[7] Applying a potential sufficiently positive to oxidize the α-TOH led to spectra with an intense absorbance at 33 550 cm^{-1}, a lower intensity absorbance at 22 100 cm^{-1} and with an isosbestic point at 42 900 cm^{-1} [Figure 4 (red lines)]. When a potential of 0 V vs Fc/Fc^+ was applied to the oxidized solutions, the spectra returned to close to that observed for the starting material, but with additional bands (or one absorbance with a shoulder) at 36 600 and 37 900 cm^{-1} [Figure 4 (dashed line)]. The additional bands at 36 600 and 37 900 cm^{-1} were also detectable during the forward oxidation cycle [Figure 4 (red lines)] but were partially obscured by the more intense absorbance at 33 550 cm^{-1}, and are likely to be associated with a decomposition/reaction product of the oxidized α-TOH such as **1** or **2** in Scheme 2.[28a] Nevertheless, the observation that the bands at 33 700 and 34 300 cm^{-1} present in the final spectrum were close in intensity to the same bands in the original (pre-electrolysis) spectrum, suggests that the additional bands (36 600 and 37 900 cm^{-1}) are due to a minor decomposition product (≤5%) whose absorbancies have high molar absorptivities compared to the bands in the α-TOH spectrum. The electrolysis reaction shown in Figure 4 was recorded over a 4-hour period with a relatively low concentration of α-TOH due to the very high sensitivity of UV−vis spectroscopy. The other spectroscopic experiments were conducted at close to the solubility limit of α-TOH in CH_3CN (~15 mM) to limit the interference caused by α-TO^+ reacting with trace amounts of water (that is present in mM concentrations).

3.3. ATR-FTIR Spectroscopy. Infrared spectra of the electrolyzed solutions were obtained using an ATR probe composed of a diamond composite material that is infrared transparent between approximately 4000−2200 cm^{-1} and 1900−650 cm^{-1},[29] which was placed in the working electrode compartment of an electrochemical electrolysis cell.[22] The initial spectrum of 15.2 mM α-TOH obtained in a background subtracted solution of CH_3CN/Bu_4NPF_6 at 243 K is shown in Figure 5b (black line). To maintain charge neutrality as the controlled potential electrolysis proceeds, the supporting electrolyte ions must transfer between the two compartments in the electrolysis cell, so that some absorbancies (positive or negative) can be assigned to the supporting electrolyte (the spectrum of Bu_4NPF_6 in a background subtracted acetonitrile solution is given in Figure 5c). Thus, the very strong absorbance that grew in at 845 cm^{-1} as the electrolysis progressed (Figure 5a) was due to the PF_6^- anion transferring from the auxiliary electrode compartment into the working electrode compartment of the electrolysis cell. Simultaneously to this occurring, the Bu_4N^+ cation transferred from the working electrode compartment into the auxiliary electrode compartment and the band between 3000 and 2850 cm^{-1} associated with the C−H stretching vibrations of the electrolyte cation decreased in size. The negative absorbance observed in the initial spectrum [Figure 5b (black line)] at 845 cm^{-1} is due to the supporting electrolyte concentration in the test solution not exactly matching the background spectrum, which is exacerbated in size due to the very high concentration of supporting electrolyte compared to analyte concentration, combined with the inherently high intensity of the absorbance.

Figure 5b (red line) is the spectrum obtained of the fully oxidized species at the end of the electrolysis, except for the absorbancies that have been attributed to the electrolyte. When a reductive potential was applied to the oxidized solution (E_{appl} = 0 V vs Fc/Fc^+) the infrared spectrum returned to close to that observed for the starting material [Figure 5b (dashed line)]. The close agreement between the initial [Figure 5b (black line)] and reverse final spectra [Figure 5b (dashed line)] provide very strong evidence that the new peaks detected in the oxidized solutions [Figure 5b (red line)] are attributable to α-TO^+, and not due to an additional reaction product, since it would be unlikely that the starting spectra would be regenerated if α-TO^+ had further reacted.

The spectrum in Figure 5b (red line) shows features that are highly supportive of the formation of the phenoxonium ion. Two new bands are detected at 1649 and 1605 cm^{-1}, which occur at a very similar wavenumber to bands observed in the spectra of nonaromatic cyclic ketones with conjugated double bonds, such as for *p*-benzoquinone derivatives.[30,31] The band at 1649 cm^{-1} is assignable to a C=O stretch and the band at 1605 cm^{-1} is consistent with a C=C ring stretch.[32] The position of these bands are supportive of the phenoxonium cation having the positive

(29) *ASI Applied Systems, Inc.*, Millersville, MD, USA (http://www.asirxn.com).
(30) C. J. Pouchert, *The Aldich Library of FT-IR Spectra*, Edition 1, Volume 1, Aldrich Chemical Co., Inc.: Milwaukee, 1985; pp 452−457.
(31) Vigalok, A.; Rybtchinski, B.; Gozin, Y.; Koblenz, T. S.; Ben-David, Y.; Rozenberg, H.; Milstein, D. *J. Am. Chem. Soc.* **2003**, *125*, 15 692−15 693.
(32) Liu, R.; Zhou, X.; Pulay, P. *J. Phys. Chem.* **1992**, *96*, 4255−4261.

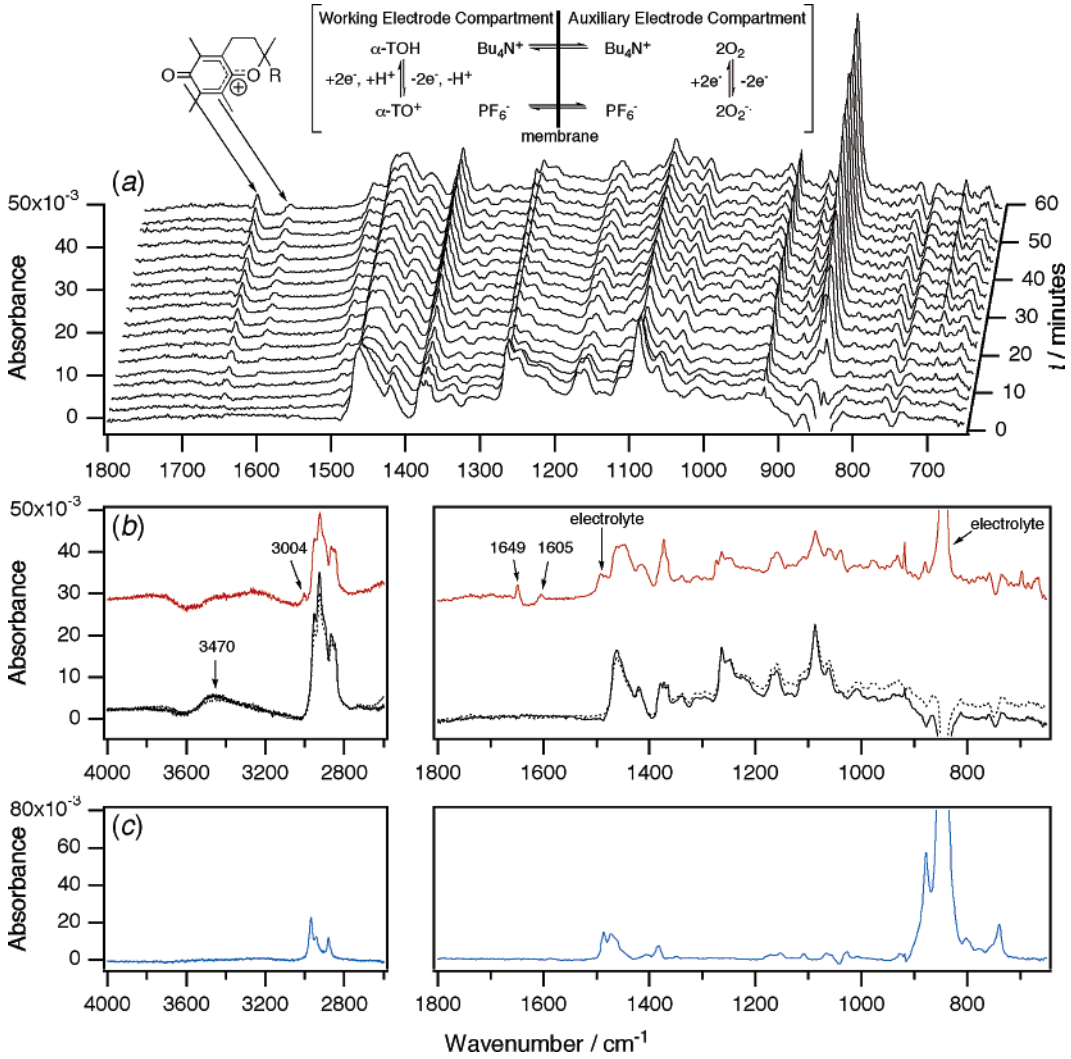

Figure 5. In situ ATR-FTIR spectra obtained at 243 K during the oxidation of 15.2 mM α-TOH at a Pt mesh electrode in CH_3CN with 0.25 M Bu_4NPF_6. (a) Sequential spectra obtained during the oxidation. (b) (Black line) Prior to the bulk oxidation of α-TOH. (Red line) After the exhaustive oxidation of α-TOH to α-TO^+ at 0.7 V vs Fc/Fc^+. (Dashed line) After the exhaustive reduction of α-TO^+ back to α-TOH at 0.0 V vs Fc/Fc^+. (c) Solution phase spectrum of 0.1 M Bu_4NPF_6.

charge localized about the carbon and oxygen atom in the para-position to the carbonyl group, thereby giving the compound a quinonoid structure (Figure 5a). This is also consistent with the final long-term products that are formed in the presence of water where a hydroxide group adds in the para-position to the carbonyl group (Scheme 2) (the IR spectrum of **2** displays a C═O stretch at 1678 cm^{-1} and a C═C stretch at 1628 cm^{-1}).[28a] The band at 1649 cm^{-1} appears somewhat less intense than often observed for a carbonyl group, but this can be accounted for by the diminishing sensitivity of the ATR probe between 1300 and 1800 cm^{-1},[29] which lowers the intensity of the higher wavenumber bands. A weak additional band was present at 3004 cm^{-1} that also appeared assignable to the α-TO^+ cation because it increased in intensity as the oxidation progressed and diminished in intensity when a reducing potential was applied.

A further feature that is supportive of the oxidized species being α-TO^+, is that the OH stretch that occurs in the neutral compound (α-TOH) at 3470 cm^{-1} [Figure 5b (black line)] is missing from the spectrum of α-TO^+ due to the formation of the carbonyl group [Figure 5b (red line)], but returns when the oxidized species is reduced back to the starting material [Figure 5b (dashed line)]. The free proton liberated during the oxidation is likely to exist as hexafluorophosphoric acid in the electrolyte rich environment without reacting irreversibly with other compounds in solution. The apparent decrease in the intensity of the C−H stretching band at 3000−2800 cm^{-1} in the spectrum of α-TO^+ [Figure 5b (red line)] is due to this band overlapping with that of the supporting electrolyte cation, which transfers from the working electrolyte compartment into the auxiliary electrode compartment as the oxidation progresses. Providing the electrolyte concentration is sufficiently high, there should be lesser transfer of the oxidized species (α-TO^+ and H^+) produced in the working electrode compartment into the auxiliary electrode compartment.

3.4. ^{1}H NMR spectroscopy. Solutions of α-TOH in CD_3CN were oxidized in an in situ electrochemical-NMR cell that used a 10 nm thick Au-film working electrode positioned within the radio frequency (RF) coils of the NMR magnet.[23] The data obtained during the electrolysis at 293 K using 0.5 M $LiClO_4$ as the supporting electrolyte are shown in Figure 6, with each spectrum representing 128 accumulated scans recorded over approximately 5 min. Within a few minutes of the oxidation potential being applied, the peaks associated with the $-CH_3$ and $-CH_2$ groups in the cyclic region of the molecule all

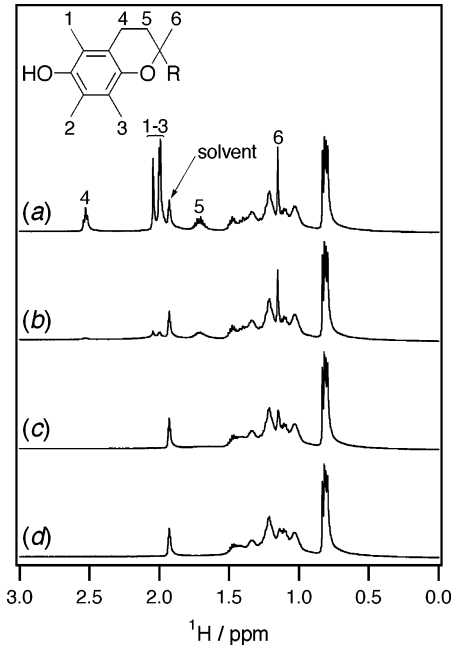

Figure 6. 500 MHz ^{1}H NMR spectra obtained at 293 K in an in situ electrochemical-NMR cell during the electrochemical oxidation of 15 mM α-TOH in CD_3CN containing 0.5 M $LiClO_4$ as the supporting electrolyte. (a) Prior to electrolysis. (b) 0−5 min. (b) 5−10 min. (d) 10−15 min.

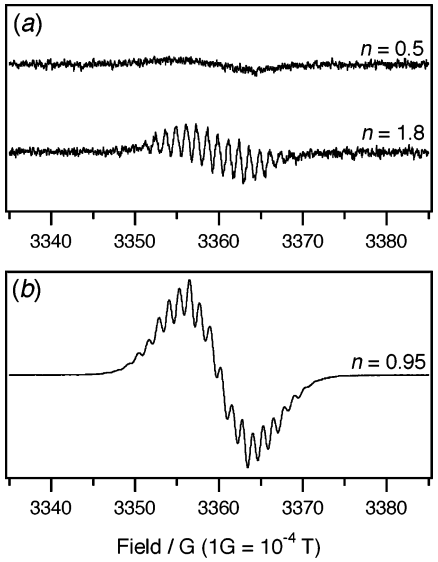

Figure 7. X-band EPR spectra obtained at 243 K during the electrolysis of (a) 10 mM α-TOH in CH_3CN with 0.25 M Bu_4NPF_6, and (b) 10 mM α-TOH and 100 mM CF_3SO_3H in CH_3CN with 0.25 M Bu_4NPF_6 to form α-$TOH^{+\bullet}$. n = the number of electrons transferred per molecule during the bulk oxidation. Microwave frequency = 9.45 GHz, modulation amplitude = 0.2 G, sweep width = 50 G, sweep time = 100 s, time constant = 100 ms, and microwave power = 20 mW. The receiver level in (*a*) is 100 times greater than the receiver level in (*b*).

diminished in intensity and could barely be detected after 10 min, while the peaks associated with the phytyl tail appeared unaffected by the electrolysis process. The peak associated with the OH group at ~5.5 ppm also disappeared (data not shown) and no new peaks were evident between 0 and 10 ppm. Previous experiments performed on halogenated aromatics indicated that the exhaustive electrolysis of 25 mM of substrate took around 1 h in the diffusion/convection controlled electrochemical-NMR cell, and the product could be seen to form within 5 min of the electrolysis commencing.[23] Therefore, the rapid disappearance of all the peaks in the cyclic portion of the molecule must be caused by broadening due to rapid electron exchange with a radical species. The phytyl tail appeared unaffected by broadening, most probably because it was sufficiently far removed from the portion of the molecule undergoing electron exchange according to the r^{-6} dependence on relaxation rate.[33] The electrolysis was also performed at 243 K using 0.25 M Et_4NPF_6 as the supporting electrolyte and the results were essentially the same as the higher temperature experiments, with the peaks due to the protons close to the cyclic portion of the molecule disappearing very shortly after the potential was first applied. [^{1}H NMR silent $LiClO_4$ has very poor solubility in CD_3CN (or CH_3CN) below ambient temperatures so is not suitable for in situ electrochemical-NMR (or FTIR) experiments at low temperatures].

3.5. EPR Spectroscopy. To test for the appearance of a radical produced during oxidation of α-TOH, in situ electrochemical-EPR experiments were performed using a channel electrode arrangement with a platinum foil electrode situated within the TE_{102} cavity of the EPR spectrometer. The cell operates by flowing fresh solution over the electrode surface so that electrogenerated species are continuously being formed then flowing out of the cavity of the spectrometer, so that a steady state EPR signal is obtained. It has been found that the channel electrode geometry is an extremely sensitive procedure for detecting electrogenerated radicals, compared to using stationary diffusion-controlled electrochemical-EPR cells.[24b] Nevertheless, when a solution of α-TOH in CH_3CN with 0.5 M Bu_4NPF_6 at room temperature was oxidized at 0.7 V vs Fc/Fc^+ in the channel flow cell, no EPR signal was detected. However, when the same solution was electrolyzed in a CPE cell at 243 K, then transferred under vacuum to an EPR tube, a weak EPR spectrum was obtained (Figure 7a). The intensity of the radical signal increased as the electrolysis progressed and when the partially electrolyzed solution was left to stand at low temperatures. When the solution was warmed to 293 K, the radical signal decayed within approximately 10 min.

The presence of a moderately stable radical in low concentrations can be accounted for by reaction 7. A consequence of reaction 7 being chemically reversible over both CV and CPE time-scales is that the proton-transfer reaction between α-$TOH^{+\bullet}$ and α-$TO^\bullet$ must also be fast and reversible. If the equilibrium

$$K_{eq} = [\alpha\text{-}TO^\bullet][H^+]/[TOH^{+\bullet}] \qquad (8)$$

strongly favored the forward process (dissociation of α-$TOH^{+\bullet}$), then on the backward electrochemical reduction step (α-TO^+ → α-TOH), the process would stop at α-$TO^\bullet$.[34] α-$TO^\bullet$ cannot be further reduced to α-TO^- until −0.9 V vs Fc/Fc^+ [Figure 1d (blue line) and Scheme 1][7,8] which is 0.9 V more negative than the reduction potential applied during the CPE experiments (0 V vs Fc/Fc^+). Furthermore, α-$TO^\bullet$ is only moderately stable in CH_3CN (especially at high concentrations) and relatively quickly decomposes by a bimolecular self-reaction ($k = 1.2 \times 10^3$ L mol^{-1} s^{-1} at 253 K[8]). Simulations[25] of the electrochemical

(33) Sanders, J. K. M.; Hunter, B. K. *Modern NMR Spectroscopy. A Guide for Chemists*, 2nd ed.; Oxford University Press: Oxford, 1993; p 163.

(34) In aqueous systems the equilibrium reaction in eq 8 may more strongly favor the dissociation reaction, since pK_a-values for phenol cation radicals are usually very acidic.

data indicate that the rate constant for the reverse chemical step (C step) in reaction 7 must be at least as fast as the bimolecular self-reaction of α-TO•, and that the equilibrium constant in reaction 8 should be ≤1. In contrast, most ECE mechanisms that have been studied by cyclic voltammetry have been found to favor the forward reactions, which are often very fast (such as during the reduction of aromatic halides[35]). Significantly, the equilibrium reaction in eq 8 will shift in the direction of α-$TOH^{+\bullet}$ as the oxidation reaction progresses due to the increase in H^+ concentration, combined with the removal of α-TO• due to its further oxidation at the electrode surface. Therefore, the EPR signal detected during the oxidation of α-TOH that was observed to increase in intensity as the reaction progressed is consistent with the α-$TOH^{+\bullet}$ cation radical. The spectrum is similar to those previously assigned to α-$TOH^{+\bullet}$ model compounds,[5,13] which display a doublet with large isotropic hyperfine coupling (ihfc) to a hydroxyl proton, smaller evenly spaced lines (~ 1 G separation) due to ihfc to other protons in the aromatic region, and with a spectral width of 22 G. The small variations between the spectra in existing reports may arise from changes in solvent composition affecting the ihfc and because the other reports deal with different model compounds. The spectrum of the other possible radical species, α-TO•,[8,12] spans a 40 G spectral width and is substantially different from the spectrum of α-$TOH^{+\bullet}$. The observation of the EPR spectrum of α-$TOH^{+\bullet}$ free from interference from the spectrum of α-TO•, indicates that the K_{eq}-value in eq 8 must be considerably <1 (possibly lower than 10^{-6}).[5]

3.6. Addition of Acid. Further evidence of the formation of α-$TOH^{+\bullet}$ came from EPR, UV−vis and electrochemical experiments performed in the presence of acid. Cyclic voltammograms obtained with increasing concentrations of CF_3SO_3H resulted in the i_p^{ox}-value decreasing, the E_p^{ox}-value shifting to more positive potentials and the ΔE_{pp}-value decreasing. The i_p^{ox}-value diminished uniformly from that of α-TOH in pure CH_3CN [Figure 8a (black line)] until approximately 0.1 M (~1% *v*/*v*) of CF_3SO_3H was added, then leveled off [Figure 8a (red line)] at close to half the i_p^{ox}-value seen for α-TOH without acid. At higher concentrations of acid above ~0.3 M the i_p^{ox}-value decreased even further but the UV−vis spectrum of α-TOH also changed in appearance indicating that decomposition had occurred (possibly due to a reaction between a breakdown product of the solvent and α-TOH). The diminishing anodic peak current at concentrations up to 0.1 M CF_3SO_3H is most likely associated with a change in the number of electrons transferred from two to one, resulting in the formation of the stable α-$TOH^{+\bullet}$ cation radical, with the reverse peak associated with the reduction of α-$TOH^{+\bullet}$ back to α-TOH. At intermediate concentrations of CF_3SO_3H (<1%), the voltammograms represent a mixture of oxidation to α-$TOH^{+\bullet}$/α-TO^+, and reduction back to α-TOH. Thus, the oxidation process at ~+1.4 V vs Fc/Fc^+ shown in Figure 8a (red line) is likely to be due to the further one-electron oxidation of α-$TOH^{+\bullet}$ to the dication, α-TOH^{2+}. Judging from the i_p^{ox}/i_p^{red} ratio, the dication appears only moderately stable (for a few seconds) in CH_3CN/CF_3SO_3H even at low temperatures. Importantly, the 0.8 V difference in potential between the α-TOH/α-$TOH^{+\bullet}$ and α-$TOH^{+\bullet}$/α-TOH^{2+} couples [Figure 8a (red line)] proves that the two-electron oxidation in neutral media to form α-TO^+ does not occur via direct electrochemical oxidation of α-TOH to the dication followed by loss of a proton (an EEC mechanism).

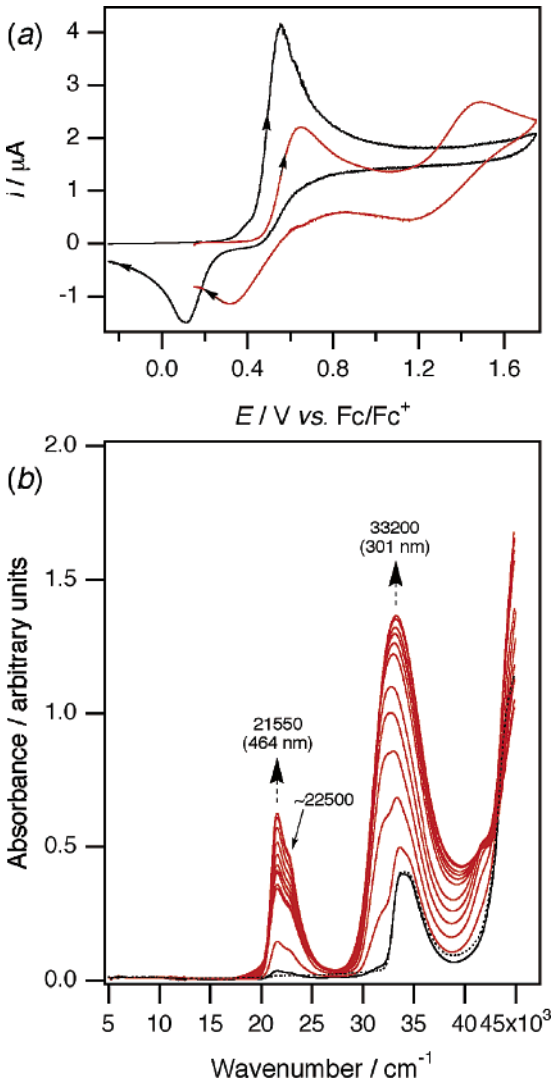

Figure 8. (a) Cyclic voltammograms recorded at 243 K at a scan rate of 0.1 V s^{-1} with a 1.0 mm diameter Pt electrode in CH_3CN with 0.25 M Bu_4NPF_6. (Black line) 2.0 mM α-TOH. (Red line) 2 mM α-TOH and 100 mM CF_3SO_3H. (b) In situ UV−vis−NIR spectra obtained at 243 K during the oxidation of 2.0 mM α-TOH at a Pt mesh electrode in CH_3CN with 0.5 M Bu_4NPF_6 and 50 mM CF_3SO_3H. (Black line) Prior to the bulk oxidation of α-TOH. (Red line) During the oxidation of α-TOH to α-$TOH^{+\bullet}$ at 0.7 V vs Fc/Fc^+. (Dashed line) After the exhaustive reduction of α-$TOH^{+\bullet}$ back to α-TOH at +0.2 V vs Fc/Fc^+.

The CV experiments described above do not provide definitive evidence that the first (least positive) oxidation and reduction processes detected in the presence of ~1−3% CF_3SO_3H are due to the one-electron oxidation of α-TOH to α-$TOH^{+\bullet}$ (and reduction of α-$TOH^{+\bullet}$ back to α-TOH). The separation between the E_p^{ox} and E_p^{red} peaks (~ 200 mV) is much wider than expected for a reversible one-electron transfer (the large ΔE_{pp}-value may partly be due to the high concentration of acid interfering with the Pt electrode surface). Convincing evidence that the first (least positive) oxidation process resulted in the formation of α-$TOH^{+\bullet}$ came from electrolysis and spectroelectrochemical experiments in the presence of acid. CPE experiments performed on solutions of α-TOH containing 0.1

(35) (a) M'Halla, F.; Pinson, J.; Savéant, J. M. *J. Electroanal. Chem.* **1978**, *89*, 347−361. (b) M'Halla, F.; Pinson, J.; Savéant, J. M. *J. Am. Chem. Soc.* **1980**, *102*, 4120−4127. (c) Wipf, D. O.; Wightman, R. M. *J. Phys. Chem.* **1989**, *93*, 4286−4291.

M CF_3SO_3H led to a yellow-green solution and the transfer of 1 ± 0.1 electrons per molecule, which substantiates the change from a two- to a one-electron process in CH_3CN containing acid. EPR experiments performed on the electrolyzed solutions gave a spectrum the same as that obtained in pure CH_3CN, but with the integrated signal intensity at least 200 times more intense (Figure 7b), which supports the assignment of α-$TOH^{+\bullet}$ as the stable one-electron oxidized product in acidic conditions. Therefore, it can be concluded that the radical detected during the electrolysis in neutral CH_3CN (Figure 7a) accounts for $<$ 0.5% of all the vitamin E species present (indicating α-$TOH^{+\bullet}$ is unlikely to have contributed to the FTIR or UV−vis−NIR spectra in Figures 4 and 5).

In situ UV−vis−NIR spectra obtained during the oxidation of α-TOH in the presence of 50 mM CF_3SO_3H are shown in Figure 8b. The oxidation process was fully chemically reversible over a period of at least 4 h at 243 K and resulted in the stable formation of α-$TOH^{+\bullet}$ (and some α-TO^+). The new band that occurred at 21 550 cm^{-1} is clearly associated with the cation radical since it is much sharper and more intense than the band that occurs at a similar wavenumber (22 100 cm^{-1}) in the spectrum of α-TO^+ (Figure 4). The band at 33 200 cm^{-1} is similar but not completely identical to that seen for α-TO^+ and represents a mixture of both α-$TOH^{+\bullet}$ and α-TO^+. When higher concentrations of acid were used during the oxidation the band around 33 000 cm^{-1} still remained but was closer in intensity to the band at 21 550 cm^{-1}. The shoulder at $\sim$22 500 cm^{-1} in the spectrum in Figure 8b is present in exactly the same ratio (with the band at 21 550 cm^{-1}) at higher acid concentrations indicating it is also associated with α-$TOH^{+\bullet}$. The observation of an absorbance around 22 000 cm^{-1} ($\sim$460 nm) in the spectra of both α-TO^+ (Figure 4) and a-$TOH^{+\bullet}$ (Figure 8b), albeit with a different shape and intensity, indicate that caution should be exercised when differentiating these species based on the UV−vis detection of transients, such as in pulse radiolysis experiments.

It was difficult to obtain well-resolved FTIR spectra of α-$TOH^{+\bullet}$ due to strong interference from CF_3SO_3H that was present in much higher concentration than α-TOH (and α-$TOH^{+\bullet}$). Nonetheless, ATR-FTIR difference spectra recorded at 243 K during the electrolysis of α-TOH using α-TOH/CH_3CN/Bu_4NPF_6/CF_3SO_3H as the background led to no new bands being detected in the 1800−1500 cm^{-1} region, confirming that the bands detected at 1649 and 1605 cm^{-1} during the oxidation in neutral media were associated with the phenoxonium ion and not the cation radical. If α-$TOH^{+\bullet}$ has any bands in the 1800−1500 cm^{-1} region, they are much less intense than those observed for α-TO^+, and may not be detectable with our present apparatus.

It is surprising that the addition of relatively small amounts of acid has a pronounced effect on the voltammetric behavior of α-TOH, allowing the detection of the monocation and at more positive potentials the dication (although this observation is also consistent with the K_{eq}-value in eq 8 being substantially <1). The addition of CF_3SO_3H to the other phenols shown in Figure 1 did not lead to a reverse peak (E_p^{red}) being detected during CV experiments at positive potentials, nor to a decrease in the i_p^{ox}-values, indicating that their associated cation radicals and phenoxonium ions were much less stable than that observed for the vitamin E system.

4. Conclusion

A combination of electrochemical (CV and CPE) and in situ spectroscopic (UV−vis−NIR, FTIR, NMR, and EPR) experiments have demonstrated that all of the redox states of α-TOH shown in Scheme 1 are accessible in CH_3CN (with Bu_4NPF_6) through the addition of appropriate concentrations of organic soluble acid (CF_3SO_3H) or base (Et_4NOH) coupled with electrochemical generation. α-TOH can be oxidized by one-electron at $\sim$+0.6 V vs Fc/Fc^+ to form α-$TOH^{+\bullet}$. In pure CH_3CN, α-$TOH^{+\bullet}$ dissociates into α-$TO^\bullet$ (and H^+), which is immediately further oxidized ($\sim$+0.2 V vs Fc/Fc^+) at the electrode surface by one-electron to form α-TO^+ (in an ECE mechanism). α-TO^+ is stable for several hours at low temperatures and can be reduced back to α-TOH on both the CV and CPE time-scales by applying 0 V vs Fc/Fc^+. The chemically reversible nature of the α-TOH/TO^+ couple is made possible by the rapid reversible equilibrium reaction that must occur between α-$TO^\bullet$ and α-$TOH^{+\bullet}$ (via the transfer of H^+) (Scheme 1 and reaction 7). In CH_3CN containing $\sim\geq$1% CF_3SO_3H the oxidation of α-TOH occurs by one-electron to form α-$TOH^{+\bullet}$. The UV−vis spectra of α-TO^+ and α-$TOH^{+\bullet}$ are similar, both displaying absorbancies at similar wavenumbers but with different shaped bands with different molar absorptivities. In acid conditions, α-$TOH^{+\bullet}$ is further oxidized at 1.4 V vs Fc/Fc^+ to form α-TOH^{2+}. Most studies on intermediate species associated with vitamin E have focused on the α-$TO^\bullet$ radical, but it is interesting to know whether α-TO^+, which has now been shown to be surprisingly stable in neutral conditions, can also play a significant role in biological redox systems, through its reversible transformation with α-TOH.

Acknowledgment. L.L.W. thanks the Research School of Chemistry for the award of a Summer Scholarship and R.D.W. thanks the Australian Research Council for the award of a QEII Research Fellowship.

JA046648J